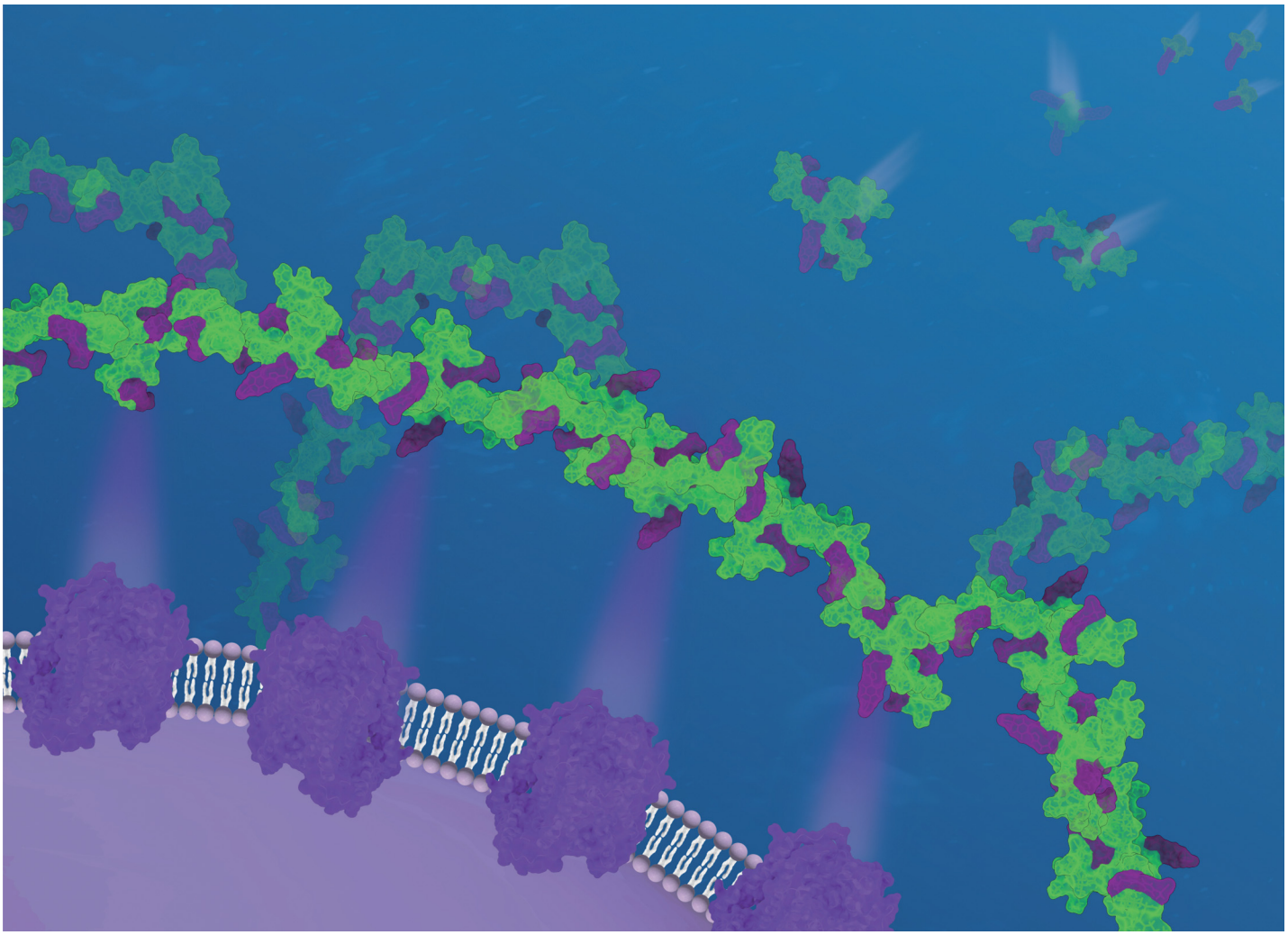

Showcasing research from Professor Matsusaki's laboratory, Division of Applied Chemistry, Graduate School of Engineering, The University of Osaka.

Fabrication of a self-assembling peptide for the inhibition of cancer cell proliferation by targeting LAT1

Self-assembling peptides targeting overexpressed proteins and/or enzymes on the cancer cell membrane have emerged as promising strategies for effective and selective cancer therapy. This work demonstrates a self-assembling peptide-based strategy to selectively suppress cancer cell proliferation *via* inhibition of L-type amino acid transporter.

Image reproduced by permission of Masahiko Nakamoto from *Chem. Commun.*, 2026, **62**, 6527.

As featured in:

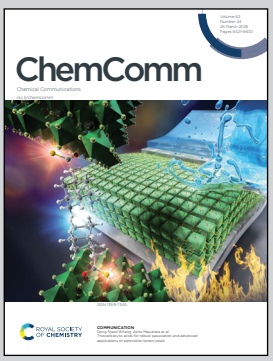

See Masahiko Nakamoto, Michiya Matsusaki *et al.*, *Chem. Commun.*, 2026, **62**, 6527.

ROYAL SOCIETY OF CHEMISTRY

rsc.li/chemcomm

Registered charity number: 207890

ChemComm

COMMUNICATION

View Article Online
View Journal | View Issue

Cite this: *Chem. Commun.*, 2026, **62**, 6527

Received 5th February 2026,
Accepted 10th March 2026

DOI: 10.1039/d6cc00782a

rsc.li/chemcomm

Fabrication of a self-assembling peptide for the inhibition of cancer cell proliferation by targeting LAT1

Yuki Koba,[a] Kanta Ogura,[a] Masahiko Nakamoto *[ab] and Michiya Matsusaki *[a]

Self-assembling peptides targeting overexpressed proteins and/or enzymes on the cancer cell membrane have emerged as promising strategies for effective and selective cancer therapy. We developed a self-assembling peptide targeting L-type amino acid transporter (LAT1), LffVLKK-4Phe, that selectively inhibits cancer cell proliferation by inhibiting LAT1. This work demonstrates a self-assembling peptide-based strategy to inhibit cancer cell proliferation *via* suppressing amino acid transport.

Overexpressed membrane-associated proteins/enzymes promote cancer cell survival and proliferation.[1–3] Therefore, nanomedicines including polymer ligands[4–8] and self-assembling peptides[9–11] that lead to cancer cell death through direct multivalent interactions with these proteins/enzymes and/or enzyme-responsive membrane disruption/intracellular stress induction have emerged as promising strategies for effective and selective cancer therapy. In this context, enzyme-responsive[12,13] or ligand-directed[14–17] self-assembling peptides that display adaptive multivalent binding interfaces with target membrane-associated proteins/enzymes can be promising for overcoming the spatial heterogeneity of cancer cells. For example, Li *et al.* reported that self-assembling peptides conjugated with a carbonic anhydrase IX (CAIX)-targeting motif inhibited cancer growth through multivalent interactions arising from nanofiber formation driven by CAIX-mediated peptide accumulation on the cancer cell membrane.[14] Recently, transporters have attracted increasing attention as promising targets for selective cancer interventions,[18,19] since they play fundamental roles in metabolic transformation and energy homeostasis through nutrient uptake.[20,21] However, to the best of our knowledge, little has been reported on self-assembling peptides that inhibit cancer cell proliferation by directly suppressing transporter-mediated substance uptake through multivalent interactions.

In this study, the L-type amino acid transporter (LAT1) was selected as the target protein because it plays an important role in the uptake of amino acids essential for proliferation.[22,23] We designed a self-assembling peptide conjugated to the L-phenylalanine (Phe) motif as an LAT1 ligand (LffVLKK-4Phe) (Fig. 1). Here, we demonstrated that LffVLKK-4Phe inhibits cancer cell proliferation by suppressing LAT1-mediated amino acid transport. The findings of this study provide a strategy for designing self-assembling peptides that inhibit cancer cell proliferation by suppressing amino acid transport.

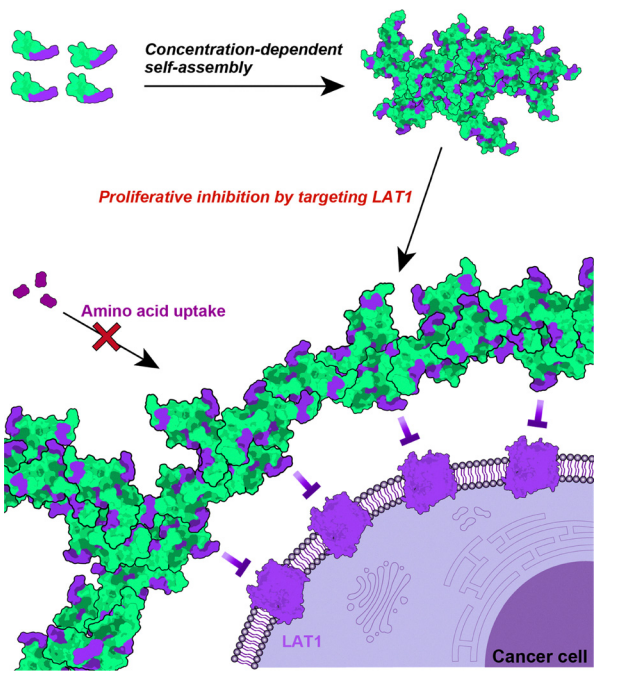

Fig. 1 (A) A Chemical structure and an illustration of a self-assembling peptide targeting LAT1, LffVLKK-4Phe. (B) Conceptual illustration of this study.

[a] *Division of Applied Chemistry, Graduate School of Engineering, Osaka University Suita, 2-1 Yamada-oka, Osaka 565-0871, Japan.*
E-mail: m-nakamoto@chem.eng.osaka-u.ac.jp, m-matsus@chem.eng.osaka-u.ac.jp
[b] *Center for Future Innovation (CFi), Faculty of Engineering, The University of Osaka, 2-1 Yamada-oka, Suita, Osaka 565-0871, Japan*

First, a self-assembling sequence[24–26] (LffVLKKalk) was synthesized by solid-phase peptide synthesis (SI 2 and Fig. S1–S3). Subsequently, 4-azido-L-phenylalanine (Phe(4-N_3)) was introduced as an LAT1-targeting motif by copper-catalyzed azide–alkyne cycloaddition, yielding LffVLKK-4Phe (SI 3 and Fig. S4–S11). The critical self-assembly concentration (CSC)[8] of LffVLKK-4Phe in Dulbecco's phosphate-buffered saline (D-PBS, pH 6.8) was determined to be 0.28 mg mL^{-1} (238 μM) based on the derived count rate from dynamic light scattering (DLS) measurements[27] (Fig. 2A). Furthermore, the dynamics arising from cooperative diffusion[28] were observed with increasing concentrations (Fig. S12A–G). These results indicated the concentration-dependent self-assembly behaviour of LffVLKK-4Phe. The hydrodynamic diameter of LffVLKK-4Phe at 0.5 mg mL^{-1} was 562.3 ± 50.5 nm (Fig. 2B). Circular dichroism (CD) spectra suggested that LffVLKK-4Phe shifted toward a β-sheet-rich secondary structure upon increasing the concentration (Fig. 2C). A decrease in $[\theta]$ values at high concentrations could be because of the light scattering and the formation of large peptide assemblies[29] (Fig. S14). The morphology of drop-cast, air-dried LffVLKK-4Phe (1.0 mg mL^{-1}) was examined by atomic force microscopy (AFM), revealing that nano-fibrous and network-like structures (Fig. 2D), whereas nanoparticle-like structures were observed at lower concentrations (0.25 and 0.5 mg mL^{-1}) (Fig. S15). The concentration-dependent self-assembly of LffVLKK-4Phe was also confirmed by fluorescence microscopy (Fig. S16). In addition, Nile red staining of the assemblies indicated that the self-assembly of LffVLKK-4Phe provided a hydrophobic environment (Fig. S17).

For further understanding, molecular dynamics (MD) simulations of peptide self-assembly were performed using GROMACS software[30] (SI 5 and Fig. S18). The LAT1 ligands of the assemblies derived from the six molecules of LffVLKK-4Phe were located outside the assembly (Fig. 2E), indicating that LffVLKK-4Phe in the assembly state could multivalently interact with LAT1. After 1 μs MD simulations, the fibrous assembly of LffVLKK-4Phe was observed (Fig. 2F). Next, the binding capacity of LffVLKK-4Phe to LAT1 was investigated through docking simulations using AutoDock Vina[31] (SI 5). The binding of LffVLKK-4Phe to the substrate pocket of LAT1 (PDB ID: 8kdn) was observed (Fig. 2G and H). The free energy change of LffVLKK-4Phe through binding was lower than that of Phe (LffVLKK-4Phe: −9.3 kcal mol^{-1}; Phe: −6.3 kcal mol^{-1}, respectively), suggesting the LAT1-targeting capability of LffVLKK-4Phe. Taken together, experimental results and simulations suggest that the self-assembly of LffVLKK-4Phe could be promoted by increasing its local concentration on the cancer cell membrane in response to the overexpression of LAT1. This assembly is expected to provide a large binding surface on the cancer cell membrane.

Next, we investigated the proliferative inhibitory effect of LffVLKK-4Phe on human breast cancer cell line, MCF-7, overexpressing LAT1,[32] under hypoxic conditions at pH 6.8[33] (SI 6). To explore the effect of the LAT1-targeting self-assembly, LffVLKKalk as a self-assembly motif alone; LffVLKK-4Phe, LffVLKK-εLys, and LffVLKK-γHA as LAT1-targeted peptides; and Phe(4-N_3) as the LAT1 ligand alone were tested (Fig. 3A and Fig. S19). Firstly, to understand the importance of LAT1 targeting, the proliferative inhibitory effect of LffVLKK-4Phe and LffVLKKalk was compared. LffVLKK-4Phe showed a considerably high proliferative inhibitory effect at 0.5 and 1.0 mg mL^{-1}

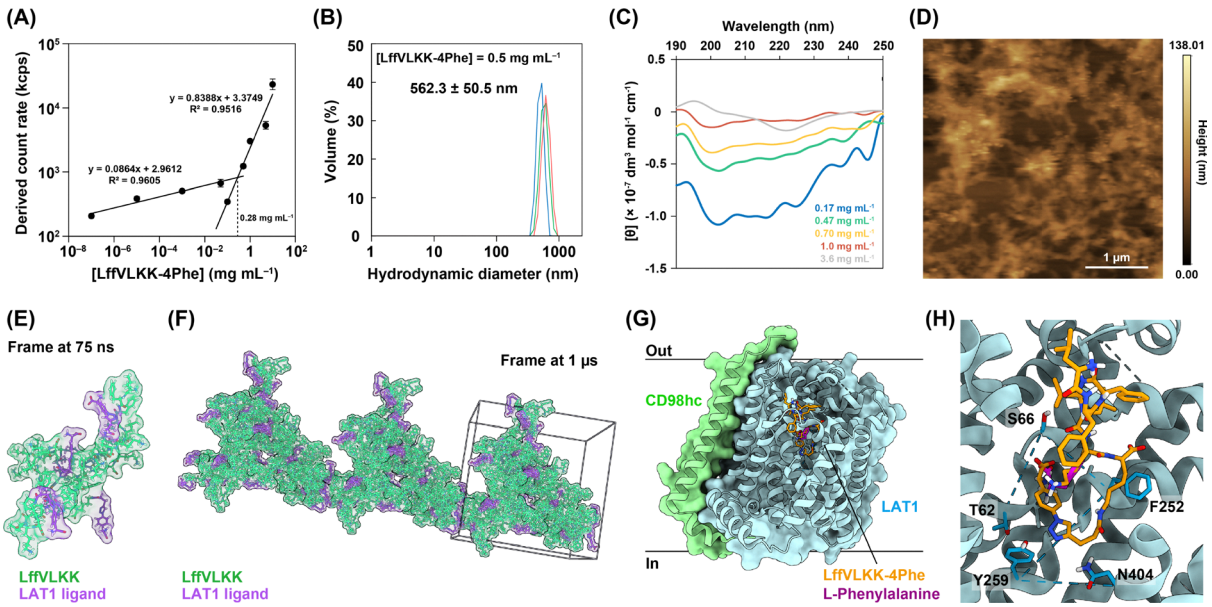

Fig. 2 (A) Derived count rate of LffVLKK-4Phe at various concentrations in D-PBS (pH 6.8). (B) Volume-based hydrodynamic diameter distribution of LffVLKK-4Phe at 0.5 mg mL^{-1}. (C) CD spectra of LffVLKK-4Phe at various concentrations in D-PBS (pH 6.8). (D) AFM image of LffVLKK-4Phe prepared at 1.0 mg mL^{-1} in 15-fold diluted D-PBS (pH 6.8). (E) Snapshot of the assemblies of LffVLKK-4Phe in MD simulations at the time point of 75 ns. (F) Snapshot of periodic copies (*z* axis) of LffVLKK-4Phe in MD simulations at the time point of 1 μs. The periodic box (8 nm × 8 nm × 8 nm) is shown in black. (G) The docked model of LffVLKK-4Phe (orange) and Phe (magenta) to LAT1. (H) Close-up views of the LffVLKK-4Phe-binding site. LffVLKK-4Phe (orange) and Phe (magenta).

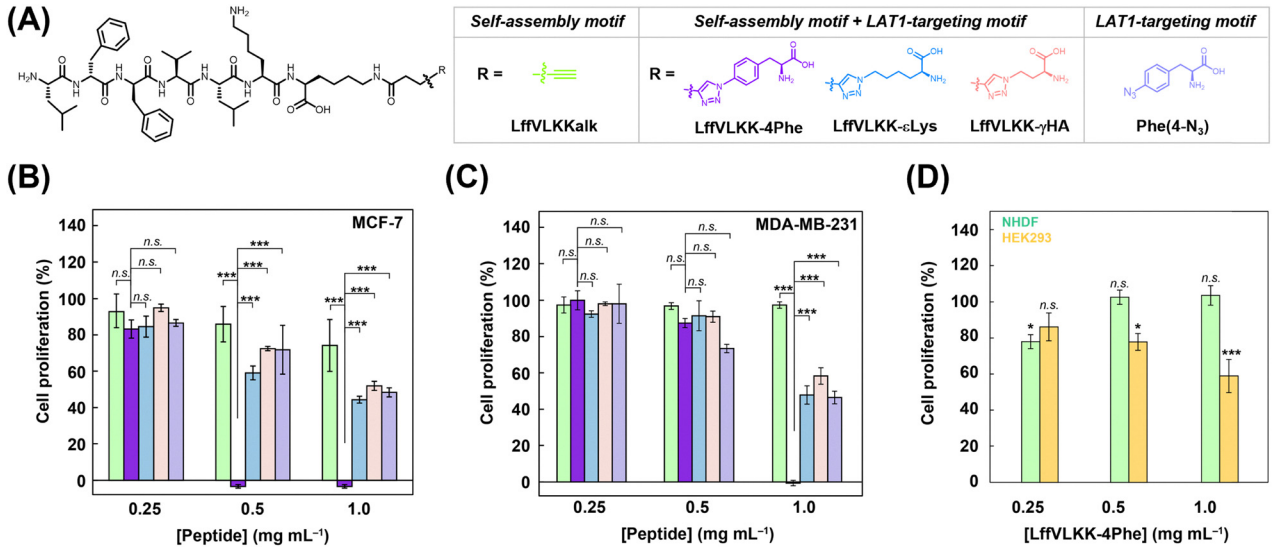

Fig. 3 (A) Chemical structure of the tested peptide ligands. LffVLKKalk as a self-assembly motif, and LffVLKK-4Phe, LffVLKK-εLys, and LffVLKK-γHA as self-assembly motif + LAT1-targeting motifs, and Phe(4-N_3) as a LAT1-targeting motif. (B, C) Cell proliferation of (B) MCF-7 and (C) MDA-MB-231 cells treated with peptide ligands and Phe(4-N_3) under hypoxic conditions for 72 h. Statistical significance was determined using one-way analysis of variance (ANOVA) followed by Tukey's post-test (n = 3) (n.s.: not significant, ***$p < 0.001$). LffVLKKalk (green), LffVLKK-4Phe (purple), LffVLKK-εLys (blue), LffVLKK-γHA (red), and Phe(4-N_3) (light purple). (D) Cell proliferation of NHDF (green) and HEK293 (yellow) treated with LffVLKK-4Phe under normoxic conditions for 72 h. Statistical significance was determined using one-way ANOVA followed by Tukey's post-test (n = 3) (n.s.: not significant, *$p < 0.05$, ***$p < 0.001$ relative to untreated cells).

after treatment for 72 h (Fig. 3B). In contrast, LffVLKKalk showed marginal efficacy at all tested concentrations (Fig. 3B) despite its comparable CSC (0.43 mg mL^{-1}) with that of LffVLKK-4Phe (Fig. S13). These results suggest that LAT1 targeting was required to inhibit MCF-7 cell proliferation. Next, to reveal the suitable structure as an LAT1 ligand, the proliferative inhibitory effect of LffVLKK-4Phe, LffVLKK-εLys, and LffVLKK-γHA were assessed. LffVLKK-4Phe exhibited significantly higher proliferative inhibition than LffVLKK-εLys and LffVLKK-γHA (Fig. 3B). In addition, the CSC of LffVLKK-4Phe in PBS was lower than those of LffVLKK-γHA and LffVLKK-εLys (0.34 mg mL^{-1} and not determined, respectively) (Fig. S13). These results suggest that the Phe motif, which is favorable for promoting self-assembly and interacting with LAT1 would be important for the effective inhibition. To understand the importance of the assembly-induced ligand multivalency, the proliferative inhibitory effect of LffVLKK-4Phe and Phe(4-N_3) were evaluated. The proliferative inhibitory effect of LffVLKK-4Phe was significantly greater than that of Phe(4-N_3) (Fig. 3B), indicating that the inhibitory effect of the LAT1 ligand could be enhanced by an increase in multivalency *via* self-assembly. Moreover, the proliferative inhibitory effect of LffVLKK-4Phe against LAT1-positive human breast cancer cell line, MDA-MB-231, was also explored, and a similar trend to that observed in MCF-7 cells was confirmed (Fig. 3C). LffVLKK-4Phe exhibited higher efficacy in MCF-7 cells than in MDA-MB-231 cells (Fig. 3C). This may be because of differences in LAT1 expression, amino acid uptake, and/or phenotype. Indeed, it has been reported that mRNA levels of LAT1 are higher in MCF-7 cells than MDA-MB-231 cells.[32] In addition, we confirmed that MCF-7 cells exhibited greater amino acid uptake than MDA-MB-231 cells (Fig. S20). Cytotoxicity in healthy cells was further evaluated using normal human dermal fibroblasts, NHDF cells, and human embryonic kidney 293, HEK293 cells, under normoxic conditions at pH 7.4. LffVLKK-4Phe did not affect cell proliferation of NHDF at any concentrations tested (Fig. 3D). Although HEK293 cell proliferation was reduced to approximately 60% at 1.0 mg mL^{-1} (Fig. 3D), cancer cell proliferation was almost completely inhibited (Fig. 3B and C). These results suggest a high selectivity LffVLKK-4Phe for cancer cells.

To elucidate the inhibitory mechanism of LffVLKK-4Phe on MCF-7 cell proliferation, amino acid uptake assays using boronophenylalanine (BPA) and lactate dehydrogenase (LDH) cytotoxicity assays were performed. At the terminal state, disrupted cell morphology was observed at 0.5 and 1.0 mg mL^{-1} (Fig. S19), implying that LffVLKK-4Phe induced cell membrane disruption in MCF-7 cells at the later stage. To gain mechanistic insights, early-stage cellular events (30 min) in MCF-7 cells were examined because the terminal stage (72 h), which is associated with complete cell death, suppresses amino acid uptake and leads to extensive LDH release. The uptake of BPA *via* LAT1 in MCF-7 cells was significantly inhibited after 30 min of treatment with LffVLKK-4Phe in a concentration-dependent manner (Fig. 4A), suggesting that LffVLKK-4Phe suppressed LAT1-mediated amino acid transport activity at an early stage of MCF-7 proliferative inhibition. At the same time point, slight increased LDH release was observed from MCF-7 cells treated with LffVLKK-4Phe (Fig. 4B). These results suggest that at an early stage, the proliferative inhibition of MCF-7 cells is predominantly caused by LAT1 inhibition, whereas membrane disruption occurs as an accompanying effect. This could be due to the self-assembly of LffVLKK-4Phe in response to the overexpression of LAT1 in the MCF-7 cell membrane.

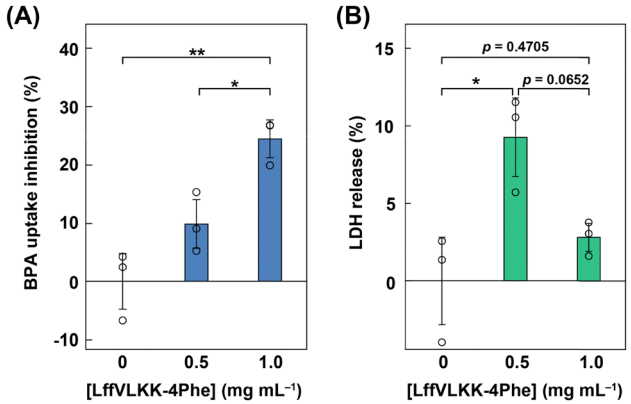

Fig. 4 (A) BPA uptake inhibition of MCF-7 cells treated with LffVLKK-4Phe for 30 min. Bar graph shows mean values. Circles indicate three independent experimental values. Data are the mean ± standard deviation (SD). (B) LDH release from MCF-7 cells treated with LffVLKK-4Phe for 30 min. Bar graph shows mean values. Circles indicate three independent experimental values. Data are the mean ± SD. Statistical significance was determined using one-way ANOVA followed by Tukey's post-test (n = 3) (*p < 0.05, **p < 0.01).

In conclusion, we developed a self-assembling peptide targeting LAT1, LffVLKK-4Phe, which selectively inhibited the proliferation of MCF-7 and MDA-MB-231 cells. These results indicated that LffVLKK-4Phe inhibited cancer cell proliferation by suppressing LAT1-mediated amino acid transport, accompanied by cell membrane disruption. The findings of this study provide a strategy for designing self-assembling peptides that can inhibit cancer cell proliferation by adapting to the spatial heterogeneity of cancer cell membranes.

Author contributions

Y. K. and M. N. designed the study, the main conceptual ideas, and the proof outline. Y. K. and M. N. designed the experiments. Y. K. and K. O. collected data. Y. K. and M. N. interpreted the data. Y. K. and M. N. wrote the manuscript. M. M. and M. N. supervised this study. All the authors discussed the results and commented on the manuscript.

Conflicts of interest

There are no conflicts to declare.

Data availability

The data supporting this article are included in the supplementary information (SI). Supplementary information is available. See DOI: https://doi.org/10.1039/d6cc00782a.

Acknowledgements

This work was supported by Grant-in-Aid for JSPS Fellows (25KJ1746), JST FOREST (JPMJFR232E), and JSPS Scientific Research for Transformative Research Areas (A) "Bottom-up Biotech" (JP 24H01137). We appreciate Dr Zhang Zhuying in The University of Osaka for AFM observations.

References

1 R. A. Cairns, I. S. Harris and T. W. Mak, *Nat. Rev. Cancer*, 2011, **11**, 85.
2 G. D. Grass, L. B. Tolliver, M. Bratoeva and B. P. Toole, *J. Biol. Chem.*, 2013, **288**, 26089.
3 H. M. Becker, *Br. J. Cancer*, 2020, **122**, 157.
4 M. Morales-Cruz, Y. Delgado, B. Castillo, C. M. Figueroa, A. M. Molina, A. Torres, M. Milián and K. Griebenow, *Drug Des., Dev. Ther.*, 2019, **13**, 3753.
5 P. Šácha, T. Knedlík, J. Schimer, J. Tykvart, J. Parolek, V. Navrátil, P. Dvořáková, F. Sedlák, K. Ulbrich, J. Strohalm, P. Majer, V. Šubr and J. Konvalinka, *Angew. Chem., Int. Ed.*, 2016, **55**, 2356.
6 Y. Koba, M. Nakamoto and M. Matsusaki, *ACS Appl. Mater. Interfaces*, 2022, **14**, 51790.
7 Y. Koba, M. Nakamoto, M. Nagao, Y. Miura and M. Matsusaki, *Nano Lett.*, 2024, **24**, 14206.
8 R. Sakamoto, Y. Koba, M. Nakamoto, T. Fukuta, K. Kadota and M. Matsusaki, *ACS Appl. Mater. Interfaces*, 2025, **17**, 59726.
9 Y. Kuang, J. Shi, J. Li, D. Yuan, K. A. Alberti, Q. Xu and B. Xu, *Angew. Chem., Int. Ed.*, 2014, **53**, 8104.
10 J. Shi, X. Du, D. Yuan, J. Zhou, N. Zhou, Y. Huang and B. Xu, *Biomacromolecules*, 2014, **15**, 3559.
11 K. Morita, K. Nishimura, S. Yamamoto, N. Shimizu, T. Yashiro, R. Kawabata, T. Aoi, A. Tamura and T. Maruyama, *JACS Au*, 2022, **2**, 2023.
12 J. Zhan, Y. Cai, S. He, L. Wang and Z. Yang, *Angew. Chem., Int. Ed.*, 2018, **57**, 1813.
13 Y. Ding, D. Zheng, L. Xie, X. Zhang, Z. Zhang, L. Wang, Z.-W. Hu and Z. Yang, *J. Am. Chem. Soc.*, 2023, **145**, 4366.
14 J. Li, K. Shi, Z. F. Sabet, W. Fu, H. Zhou, S. Xu, T. Liu, M. You, M. Cao, M. Xu, X. Cui, B. Hu, Y. Liu and C. Chen, *Sci. Adv.*, 2019, **5**, eaax0937.
15 J. Li, Y. Fang, Y. Zhang, H. Wang, Z. Yang and D. Ding, *Adv. Mater.*, 2021, **33**, 2008518.
16 M.-D. Wang, G.-T. Lv, H.-W. An, N.-Y. Zhang and H. Wang, *Angew. Chem., Int. Ed.*, 2022, **61**, e202113649.
17 H. Yin, Y. Hua, S. Feng, Y. Xu, Y. Ding, S. Liu, D. Chen, F. Du, G. Liang, W. Zhan and Y. Shen, *Adv. Mater.*, 2024, **36**, 2308504. (ligand for ALX, conc.).
18 X. Wu, J. Shen, X. Jiang, H. Han, Z. Li, Y. Xiang, D. Yuan and J. Shi, *Chem. Eng. J.*, 2024, **493**, 152479.
19 Y. Lee, C. Jin, R. Ohgaki, M. Xu, S. Ogasawara, R. Warshamanage, K. Yamashita, G. Murshudov, O. Nureki, T. Murata and Y. Kanai, *Nat. Commun.*, 2025, **16**, 1635.
20 Z. C. Nwosu, M. G. Song, M. P. di Magliano, C. A. Lyssiotis and S. E. Kim, *Oncogene*, 2023, **42**, 711.
21 R. Xia, H.-F. Peng, X. Zhang and H.-S. Zhang, *Int. J. Biol. Macromol.*, 2024, **260**, 129646.
22 Y. Kanai, H. Segawa, K. Miyamoto, H. Uchino, E. Takeda and H. Endou, *J. Biol. Chem.*, 1998, **273**, 23629.
23 P. Häfliger and R.-P. Charles, *Int. J. Mol. Sci.*, 2019, **20**, 2428.
24 D. Iglesias, M. Melle-Franco, M. Kurbasic, M. Melchionna, M. Abrami, M. Grassi, M. Prato and S. Marchesan, *ACS Nano*, 2018, **12**, 5530.
25 G. Chen, T. Xu, Y. Yan, Y. Zhou, Y. Jiang, K. Melcher and H. E. Xu, *Acta Pharmacol. Sin.*, 2017, **38**, 1205.
26 S. Marchesan, L. Waddington, C. D. Easton, D. A. Winkler, L. Goodall, J. Forsythe and P. G. Hartley, *Nanoscale*, 2012, **4**, 6752.
27 K. Moroishi, M. Nakamoto, S. Fujita, M. Kawahara, R. Katayama and M. Matsusaki, *Mater. Today Bio*, 2026, **37**, 102752.
28 T. Kureha, H. Minato, D. Suzuki, K. Urayama and M. Shibayama, *Soft Matter*, 2019, **15**, 5390.
29 J. Kardos, M. P. Nyiri, É. Moussong, F. Wien, T. Molnár, N. Murvai, V. Tóth, H. Vadászi, J. Kun, F. Jamme and A. Micsonai, *Protein Sci.*, 2025, **34**, e70066.
30 M. J. Abraham, T. Murtola, R. Schulz, S. Páll, J. C. Smith, B. Hess and E. Lindahl, *SoftwareX*, 2015, **1–2**, 19.
31 O. Trott and A. J. Olson, *J. Comput. Chem.*, 2010, **31**, 455.
32 D. B. Shennan, J. Thomson, I. F. Gow, M. T. Travers and M. C. Barber, *Biochim. Biophys. Acta, Biomembr.*, 2004, **1664**, 206.
33 O. Warburg, F. Wind and E. Negelein, *J. Gen. Physiol.*, 1927, **8**, 519.

